Official journal of the JHL 2689-9620
www.light-am.com

Review Open Access

Resolution enhancement of digital holographic microscopy via synthetic aperture: a review

Peng Gao[1,2,*] and Caojin Yuan[3,*]

Abstract

Digital holographic microscopy (DHM), which combines digital holography with optical microscopy, is a wide field, minimally invasive quantitative phase microscopy (QPM) approach for measuring the 3D shape or the inner structure of transparent and translucent samples. However, limited by diffraction, the spatial resolution of conventional DHM is relatively low and incompatible with a wide field of view (FOV) owing to the spatial bandwidth product (SBP) limit of the imaging systems. During the past decades, many efforts have been made to enhance the spatial resolution of DHM while preserving a large FOV by trading with unused degrees of freedom. Illumination modulation techniques, such as oblique illumination, structured illumination, and speckle illumination, can enhance the resolution by adding more high-frequency information to the recording system. Resolution enhancement is also achieved by extrapolation of a hologram or by synthesizing a larger hologram by scanning the sample, the camera, or inserting a diffraction grating between the sample and the camera. For on-chip DHM, spatial resolution is achieved using pixel super-resolution techniques. In this paper, we review various resolution enhancement approaches in DHM and discuss the advantages and disadvantages of these approaches. It is our hope that this review will contribute to advancements in DHM and its practical applications in many fields.

Keywords: Digital holographic microscopy, Resolution enhancement, Computational imaging, Illumination modulation

Introduction

Optical microscopy is a powerful tool for detecting subtle structures of samples, playing an irreplaceable role in many fields. However, traditional optical microscopy can only obtain the amplitude information of samples, and transparent samples, such as living cells cannot be investigated. Although fluorescence microscopy can selectively render and highlight the structures of interest by prior tagging with fluorescent markers, the phototoxicity and photobleaching of fluorescence tagging make it difficult to continuously observe living cells over a long time. Thus, there is an urgent need for label-free microscopic tools able to follow organelles in live cells. Digital holographic microscopy (DHM) [1–6], which combines digital holography and microscopy, is a label-free, quantitative phase microscopy approach. A typical setup for DHM is shown in Fig. 1a, in which a magnified object wave and a reference wave interfere with each other, and the generated off-axis hologram or phase-shifting

Correspondence: Peng Gao (peng.gao@xidian.edu.cn) or Caojin Yuan (yuancj@njnu.edu.cn)
[1]School of Physics and Optoelectronic Engineering, Xidian University, Xi'an 710071, China
[2]Academy of Advanced Interdisciplinary research, Xidian University, Xi'an 710071, China
Full list of author information is available at the end of the article.

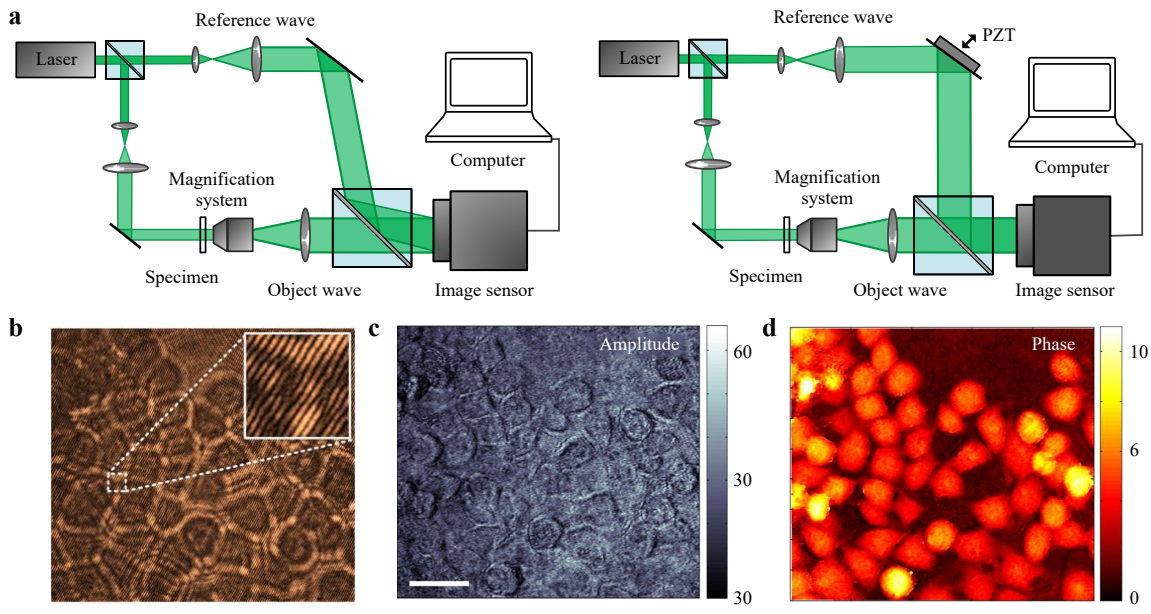

Fig. 1 Principle of digital holographic microscopy (DHM). **a** Schematic setup of off-axis (left) and in-line DHM (right). **b** Exemplary hologram of off-axis DHM. **c**, **d** Amplitude and phase images of HeLa cells reconstructed from **b**. Scale bar in **c** is adapted with permission from Ref. 76 ©The Optical Society.

holograms are recorded by a CCD camera. From the off-axis hologram (Fig. 1b), both the amplitude and phase images (Fig. 1c, d) of a sample can be obtained simultaneously. As an alternative, inline lensless DHM can help recover the phase information with an iterative algorithm without using an independent reference wave[7,8]. Refocusing of the reconstructed images can further be performed digitally using the obtained complex amplitude of the object wave[9,10]. In general, DHM can not only observe transparent samples with high endogenous contrast, but also quantitatively assess the thickness or refractive index distributions of these samples. Therefore, DHM has been widely applied in industrial inspection[11,12], visualization of liquid/gas flows[13], biomedical imaging[14], etc.

The spatial resolution is of great importance for DHM because it determines the smallest structures that can be resolved. As illustrated in Fig. 2a, when two infinitely small points separated by a Rayleigh distance of 0.61λ/NA are imaged by a diffraction-limited imaging system, two Airy patterns are generated in the imaging plane, whose complex amplitudes are denoted as O_1 and O_2, respectively. Here, λ and NA indicate the illumination wavelength and the sum numerical aperture (NA) of the imaging system (NA_{imag}) and illumination system (NA_{illum}), respectively. For incoherent illumination, the intensity of the image is linearly related to the intensity emitted from the sample, that is, $|O_1|^2+|O_2|^2$. The two patterns are considered to be resolved if the center of the intensity pattern of O_1 coincides with the first zero of the pattern of O_2 (Fig. 2b). For coherent imaging (e.g., DHM), a linear relationship holds between the input complex amplitude and the output complex amplitude. In this case, the intensity of the image corresponds to $|O_1+O_2|^2$, which is dependent on the phase difference $\Delta\varphi$ between O_1 and O_2. It is evident from Fig. 2c that for $\Delta\varphi = 0$ (in-phase), the Airy patterns of O_1 and O_2 are considered unresolved. However, for $\Delta\varphi = \pi$ (anti-phase), the Airy patterns of O_1 and O_2 are well separated. To conclude, there is no easy criterion for evaluating the resolution of coherent microscopy (DHM), considering that the resolution depends on both the microscope and the phase of the sample. Nevertheless, we recommend the following:

$$\sigma = \frac{\kappa_1 \lambda}{NA} = \frac{\kappa_1 \lambda}{NA_{\mathrm{imag}} + NA_{\mathrm{illum}}} \quad (1)$$

for evaluating the resolving power of optical microscopy. Factor κ_1 is determined by the experimental parameters, such as the coherent noise level and the SNR of the detector, etc[3,15]. Herein, we assign $\kappa_1 = 0.82$[16,17], for which the principal intensity maximum of pattern O_1 coincided with the first minimum of the in-phase O_2. This suggests two options for enhancing the spatial resolution of the DHM. The first is the use of a shorter wavelength, for example, 193-nm[18] light was used to enhance the spatial resolution of the DHM. The other is to enlarge the NAs of both the illumination and the recording systems.

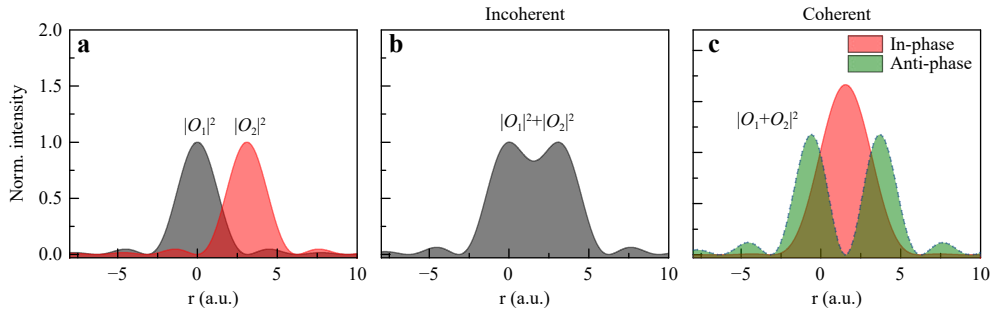

Fig. 2 Resolution criteria in incoherent and coherent systems. **a** Intensity distribution of the Airy patterns for the complex amplitude distributions, O_1 and O_2, obtained by imaging two infinitely small point sources through a diffraction-limited system; the superimposed intensities of O_1 and O_2 in incoherent microscopy **b** and coherent microscopy **c**. In-phase and anti-phase in **c** indicates that the cases O_1 and O_2 have a phase difference of 0 and π, respectively.

In addition to the resolution, the field of view (FOV) is also a vital parameter of an imaging system. The ratio between these two parameters determines the space-bandwidth product (SBP) of the imaging system[19,20]. Often, a DHM system has a limited SBP, and consequently, there is an inherent trade-off between resolution and FOV. This means that a reconstructed image with a higher resolution has a smaller FOV. Just as an example, a standard 20 × /0.4 microscope lens with a resolution limit of 0.8 μm and a circular FOV of 1.1 mm in diameter, provides a SBP of ~7 megapixels[21]. However, microscopists always expect to have a higher SBP in the sense of an increasing resolution while maintaining FOV. There are many degrees of freedom, including spatial/temporal resolution, FOV, polarization, spectrum, etc., in an imaging system. We can convert or trade some unused degrees of freedom (e.g., time) for an increase in SBP. In the past few decades, computational microscopy methods have emerged, generating images with high resolution and a wide FOV by using modulated illumination or applying other physical manipulations during the imaging process. By synthesizing apertures using the object information obtained under different modulation/manipulation operations, the SPB limitation of conventional microscopes (including DHM) can be bypassed[22,23].

This paper aims to review the resolution enhancement approaches of DHM, which are classified into three types: 1. Enlarging the NA of illumination via oblique illumination, structured illumination, and speckle illumination; 2. Enlarging the NA of the recording system via hologram extrapolation, hologram expansion, and pixel super-resolution. 3. Artificial intelligence (AI) assistance resolution enhancement approaches for DHM. This paper will cover the basic principles, implementation schemes, and exemplary results of the different approaches. We conclude by providing a summary and future outlook of resolution-enhancement approaches for DHM.

Results

Enlarging the NA of illumination

A microscopic imaging system is commonly introduced to DHM, which provides a magnified and high-resolution image of the sample. A plane wave is often used for illumination, and only the spatial frequencies diffracted by the sample up to ~ $NA_{\mathrm{imag}}/\lambda$ can be transmitted through the limited aperture of the microscope lens (Fig. 3a, *upper part*), resulting in an upper limit for the spatial resolution in terms of $0.82\lambda/NA_{\mathrm{imag}}$. Therefore, using oblique illumination, structured illumination, or speckle illumination to provide a NA_{illum} is an effective method for further improving the resolution.

DHM with oblique illumination

Since the first implementations of oblique beam illumination in DHM in the 1970s[24–27], many approaches have been extensively reported on for replicating a larger aperture[28–48]. When a sample is illuminated by an oblique wave, the high spatial frequency of the object wave in the opposite direction of the oblique illumination will be downshifted and, thus, will pass through the limited aperture of the imaging system (Fig. 3a, *lower part*). The downshifted frequencies are back-assembled to their original positions in the spectrum of the object, thus, synthesizing a wider spectrum than that of the NA-defined aperture[31]. The final resolution-enhanced image is obtained by an inverse Fourier transform (FT) of the synthesized spectrum. In comparison with conventional lens-based DHM with a resolution limit of 0.82λ/NA, DHM with oblique beam illumination has an enhanced spatial resolution, as described in Eq. 1.

Kuznetsova et al. and Schwarz et al. used oblique beam illumination to downshift the high-frequency components

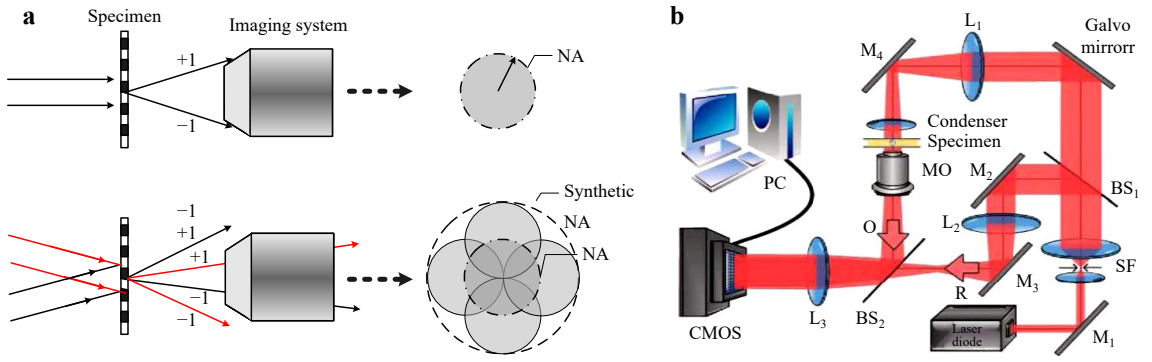

Fig. 3 DHM with oblique illumination. **a** Schematic of synthetic aperture via oblique illumination in different orientations. **b** schematics of setup of off-axis DHM with oblique illumination. Fig. 3b is adopted from Ref. 49.

of the spectrum of the object, and introduced a conjugate carrier phase to upshift the spectrum content back to its proper region[28,50]. This process was repeated sequentially for both the *x*- and *y*-illumination directions, thus allowing for the transmission of extended frequency bandwidths of the 2D object, yielding a resolution gain with a factor of three. Mico et al. utilized a vertical-cavity surface-emitting laser (VCSEL) array to generate multi-directional oblique illumination of DHM and retained a resolution gain with a factor of five[47]. The use of scanning elements has also been reported as a technological improvement for providing more flexible oblique beam illumination[28,33,37,51], which has also been validated[29,31,52] in comparison with the tilting of the illumination direction. For instance, Cheng et al. used a 2D Galvo-scanner to generate oblique illumination for DHM (Fig. 3b), achieving a two-fold isotropic resolution enhancement. [49] Oblique beam illumination for resolution enhancement has also been implemented using a spatial light modulator (SLM) [53–55] or a fiber bunch[56–60]. Meanwhile, single-shot synthetic aperture DHM was realized by using an SLM to generate multiple non-coplanar illumination beams, and using coherence gating to avoid self-interference between these non-coplanar beams[53]. Moreover, wavelength multiplexing techniques[34–36] were utilized to perform multiple oblique illuminations during a single exposure. Oblique beam illumination techniques have recently been implemented in a commercial upright Olympus microscope[39]. Notably, the maximum synthetic numerical aperture is limited by NA<1 in imaging systems with dry objectives, and further resolution improvements to λ/3.7 were demonstrated using evanescent waves[29]. In addition, axial rather than transversal resolution improvement has also been validated by SA generation[61], and an application of the technique to edge processing was also reported[62]. It is interesting to mention that oblique illumination has also been applied to differential interference contrast (DIC) microscopy[63] and Zernike phase contrast microscopy[64].

Recently, oblique illumination was also applied to obtain 3D refractive index (RI) tomographic images of transparent or translucent samples via optical diffraction tomography (ODT)[49,65]. ODT enables the probing of 3-D RI maps of a sample by recording the complex wavefront diffracted while rotating the sample[66,67] or varying illumination angles[68,69]. Kim[68] adapted DHM to ODT by using a 2D galvanometric mirror to generate different illumination directions and consequently, reconstructed a 3D RI distribution of the samples with high lateral and axial resolutions. Ozcan[70] presented an on-chip ODT scheme that enables the imaging of a large volume of approximately 15 mm^3, with a spatial resolution of < 1 μm ×1 μm × 3 μm. In 2020, Wang et al.[71] reported a mechanical-scanning-free ODT configuration using self-accelerating Airy beams that are tilted along the beam path direction, providing a 3D volumetric view of the cells. Recently, Kus et al.[72] proposed a real-time ODT system for recording a complete set of projections in a single hologram in a multiplexing manner by using a microlens, with which the tomographic images of living cells and flow cytometry could be observed clearly. In addition to advances in ODT hardware, artificial intelligence (AI)-based reconstruction algorithms have been reported to reduce the recording time and improve the quality of the reconstructed images[73].

DHM with structured illumination (SI)

Structured illumination microscopy (SIM) is a super-resolution optical microscopy technique that has the merits of being fast, minimally invasive, and has no requirement for fluorescent labeling[74,75]. Compared with conventional wide-field (WF) microscopy, SIM provides two-fold spatial resolution enhancement by illuminating the sample with a periodic pattern and recording the generated moiré pattern. Because of the moiré effect, the high spatial

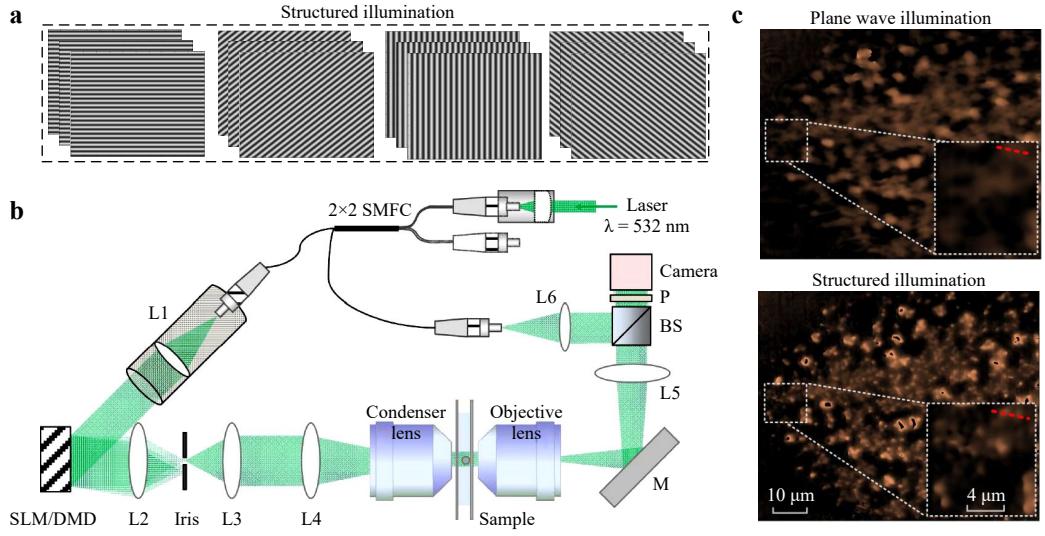

Fig. 4 DHM with structured illumination. **a** Schematic of structured illumination with different orientations and phase shifts. **b** Schematic setup of DHM with structured illumination. **c** Experimental results for resolution enhancement. Reconstructed phase images using plane wave illumination (top) and structured illumination (bottom). **b** is adopted from Ref. 77. and **c** is adopted from Ref. 76.

frequency components of the sample, which are not accessible in conventional microscopy, are shifted into the detectable domain and thus can be observed. However, the application of SIM has been limited to fluorescent samples. In 2010, Mudassar and Hussain[60] applied it to non-fluorescent scattering imaging, for which fringe patterns were generated by the interference between the beams carried by two fibers.

A DHM with structured illumination generated by an electric modulation device has been proposed. The fringe patterns were generated by a spatial light modulator (SLM)[76] in 2013 and by a digital micromirror device (DMD)[77] in 2015, whereby fringes with different orientations and phase shifts were projected without mechanical motion. In the implementation, four binary phase gratings rotated by m×45° (Fig. 4a) and generated by an SLM or a DMD are projected onto the sample, so that the sample is illuminated sequentially by four sinusoidal fringe patterns. After passing through a telescope system comprised of the microscope objective *MO* and lens *L*, the object wave interferes with a tilted reference wave *R*, and the generated holograms are recorded by a CCD camera, as shown in Fig. 4b. We denote with Ψ_{mn} the object wave generated by illuminating the sample with the grating as having the *m*-th orientation and *n*-th phase shifting. Thus, the recorded hologram can be described as $I_{mn} = |R + \Psi_{mn}|^2$. From this intensity, the wave Ψ_{mn} can be reconstructed using standard reconstruction methods, as in off-axis DHM. Generally, Ψ_{mn} can be decomposed into three components, $A_{m,-1}$, $A_{m,0}$, and $A_{m,1}$ corresponding to the -1^{st}, 0th, and $+1^{st}$ diffraction orders of the illumination wave. When we assume that the phase shift increment for each shifting of the grating is α, Ψ_{mn} can be written as:

$$\Psi_{mn} = \gamma_{-1}\exp(-in\alpha)A_{m,-1} + \gamma_0 A_{m,0} + \gamma_1\exp(in\alpha)A_{m,1} \quad (2)$$

where γ_{-1}, γ_0, and γ_1 denote the magnitudes of the diffraction orders. From Eq. 2, we can calculate the reconstructed object waves $A_{m,-1}$, $A_{m,0}$, and $A_{m,1}$ from the different diffraction orders:

$$\begin{bmatrix} A_{m,-1} \\ A_{m,0} \\ A_{m,1} \end{bmatrix} = \begin{bmatrix} \gamma_{-1}\exp(-i\alpha) & \gamma_0 & \gamma_1\exp(i\alpha) \\ \gamma_{-1}\exp(-i2\alpha) & \gamma_0 & \gamma_1\exp(i2\alpha) \\ \gamma_{-1}\exp(-i3\alpha) & \gamma_0 & \gamma_1\exp(i3\alpha) \end{bmatrix}^{-1} \cdot \begin{bmatrix} \Psi_{m1} \\ \Psi_{m2} \\ \Psi_{m3} \end{bmatrix} \quad (3)$$

Then, $A_{m,-1}$ and $A_{m,1}$ under each illumination direction are compensated for by the carrier phase due to the tilted propagation direction along the $\pm 1^{st}$ diffraction orders, and synthesized together with $A_{m,0}$ in the Fourier plane to yield the synthetic spectrum. Finally, a focused image with enhanced resolution was retrieved by the inverse FT of the synthetic spectrum. Assuming that the angular aperture of the imaging system is NA_{imag}, the synthetic *NA* of the SI DHM is $NA = NA_{imag} + \sin\theta_{illum}$. Here, θ_{illum} denotes the illumination angle of the +1 or −1 diffraction orders, and the highest value of the $\sin\theta_{illum}$ is, in turn, determined by the NA of the condenser lens. Fig. 4c validates the resolution enhancement of the structured illumination in comparison with on-axis illumination. Of note, the phase image at the bottom (obtained with structured illumination) has a better resolution compared with that on the top, and the two particles separated by 1.4 μm became

distinguishable.

Recently, structured illumination has been widely applied to different variations of DHM for the purpose of imaging transparent samples with resolution enhancement[76–89]. SI-based DHM was extended for resolution enhancement in the axial direction, aside from the lateral directions[90]. An iterative reconstruction algorithm, as well as a PCA-based algorithm, were employed to obtain resolution-enhanced images using structured illumination with unknown phase shifts or free of phase shifts[82–84, 89]. In 2021, an end-to-end deep-learning-based method, DL-SI-DHM, was proposed for improving the reconstruction efficiency and accuracy of SI-DHM[91]. In addition to synthetic-aperture phase imaging, Shin et al. in 2015 and Chowdhury et al. in 2017 utilized DMD- and SLM-based structured illumination to obtain 3D refractive index tomographic images of samples[77,92].

DHM with speckle illumination

Speckle illumination has been known since the invention of the laser in 1960[93]. Speckle illumination often reduces the signal-to-noise ratio (SNR) in coherent imaging. Speckle fields can be understood as a combination of plane waves with various random illumination directions. These oblique plane waves shift the spectrum of the object in the reciprocal plane, allowing for access to additional spatial frequencies. Thus, speckles can be used to enhance the spatial resolution and reduce the coherent noise in DHM or other coherent imaging[37, 94–97].

Fig. 5 shows the optical setup of DHM with a speckle illumination according to Ref. 95. The speckle field was generated by an SLM and projected using a telescopic system L_1-MO_1 in the sample plane, where $A^i_{S\,speckle}$ is the ith speckle illumination and A^i_o refers to the complex amplitudes of the object wave when the sample was illuminated with $A^i_{S\,speckle}$. When A^i_o interferes with a reference wave R, the hologram can be denoted as $I^i_o = |A^i_o + R|^2$. The complex amplitude of the speckle field $A^i_{S\,speckle}$ can be reconstructed from the hologram recorded in the absence of a sample. Often, the holographic resolution-enhanced image can be obtained by averaging multiple angle-dependent E-field images $O_{\mathrm{ave}} = 1/\mathrm{N}\sum_{i=1}^{N} A^i_o/A^i_{S\,speckle}$[96]. It is worth mentioning that the resolution enhancement capability of such an averaging operation will be lower when the speckle field has an unequal weight or power over the entire frequency spectrum.

To overcome this limitation, an iterative reconstruction method[95] was proposed for synthesizing a larger NA. The key idea of the iteration is to propagate the object wave between the image plane and the CCD plane, updating the speckle illumination in the image plane and the object wave intensity (with the recorded one) in the CCD plane. The iterative method enhances not only the resolution but also the SNR when the reconstructed object wavefronts from different speckle-based holograms are averaged. Utilizing SLM for speckle field illumination avoids mechanical movements and allows for a high repeatability in comparison with dynamic devices. Time-changing speckle illumination is similar to structured illumination. The concept in common is the encoding of an object with an a priori known high-resolution pattern that folds the high spatial frequencies into the low bandwidth range. The decoding patterns should be matched to the time-changing encoding patterns.

Similar to speckle illumination, a scattering medium can also be placed before the sample to enhance the spatial resolution and FOV[98,99]. Multiple scattering of the medium is a deterministic process that is described by a transmission matrix (TM) in transmission geometry. TM-based imaging has been introduced in DHM, yielding an improved resolution beyond what an objective-lens-based imaging system can achieve[99]. Similarly, a single

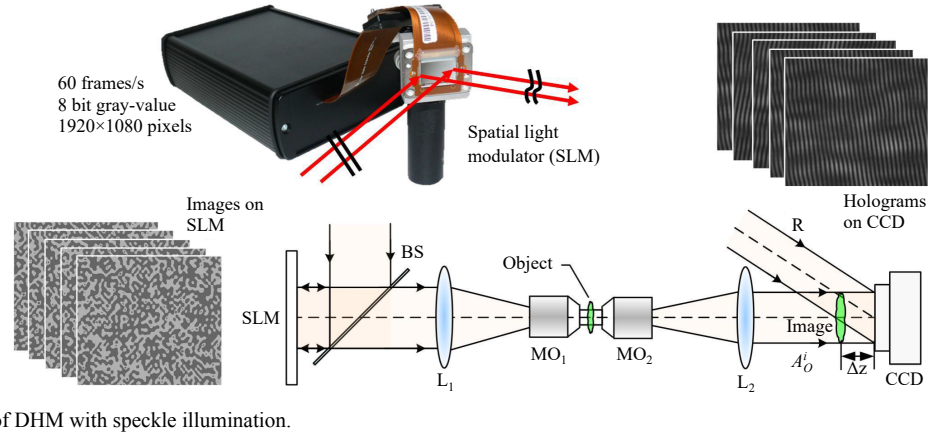

Fig. 5 Schematic of DHM with speckle illumination.

multimode optical fiber was demonstrated for scanner-free and wide-field endoscopic imaging[96]. Beyond resolution enhancement, Baek et al. demonstrated in 2018 that a high-resolution, long working distance, reference-free DHM can be performed by using a scattering layer to replace the conventional imaging lens[100]. By exploiting the randomness of a multiple-scattering layer, it allows for holographic imaging of a microscopic object without introducing a reference beam. The authors experimentally demonstrated a high NA (0.7) with a working distance of 13 mm.

Enlarging the NA of DHM recording systems

Compared to DHM with an imaging system, DHM without using an imaging lens (lens-free DHM) possesses three significant advantages. The first aspect is its compactness and low-cost because it does not employ an objective. The second is a large FOV. The third is the high compatibility and ease of integration with microfluidic and on-chip devices. In the following sections, we review the resolution enhancement of lens-free DHM via hologram extrapolation, hologram synthesis, and pixel super-resolution techniques.

Hologram extrapolation

As a major type of lens-free DHM, lensless DHM can be traced back to an inline architecture proposed by Gabor[8]. In Gabor, in lensless DHM[8,101,102] (Fig. 6a) a sample is illuminated by a spherical wave. The wave diffracted by the sample interferes with the non-diffracted wave, which also acts as a reference wave. Direct reconstruction of the generated hologram suffers from overlapping of the DC term and the twin image. Iterative approaches[7,103,104], and compressive sensing[105] have been invented to retrieve phase information from an oversampled diffraction pattern. The achievable spatial resolution is believed to be limited by the size of the hologram[8,104]:

$$\sigma = \frac{\lambda z}{N\Delta_S} \tag{4}$$

where λ is the wavelength, z is the distance between the object and the screen, N is the number of pixels, and Δ_S is the pixel size of the detector. In 2013, resolution enhancement of lensless DHM was reported by extrapolation of the hologram[104], and later, this method was applied to terahertz inline lensless holography[106,107]. The flowchart of the resolution enhancement routine is shown in Fig. 6b, and includes the following steps:

(1) Initialize the object wave $U(x_S, y_S)$ in the hologram plane by taking the square root of the hologram intensity H_0 of $N_0 \times N_0$ and padding it with zeros to a matrix of $N \times N$ with $N > N_0$ (see Fig. 6a$_1$). In contrast, random noise can be added to the padded area.

(2) Propagate the padded wave $U(x_S, y_S)$ to the object plane by using the propagation integral[7], yielding $o(x_o, y_o)$.

(3) In the object plane, a constraint concerning the finite size and positive absorption of the sample is applied to $o(x_o, y_o)$, resulting in $o'(x_o, y_o)$.

(4) Propagate $o'(x_o, y_o)$ in the hologram plane and replace the amplitude of $o'(x_o, y_o)$ with the square root of the hologram intensity $H0$ within the central $N_0 \times N_0$ area (see Fig. 6a$_2$).

Once the above procedures have been repeated over 500 iterations, the complex amplitude of the object wave can be

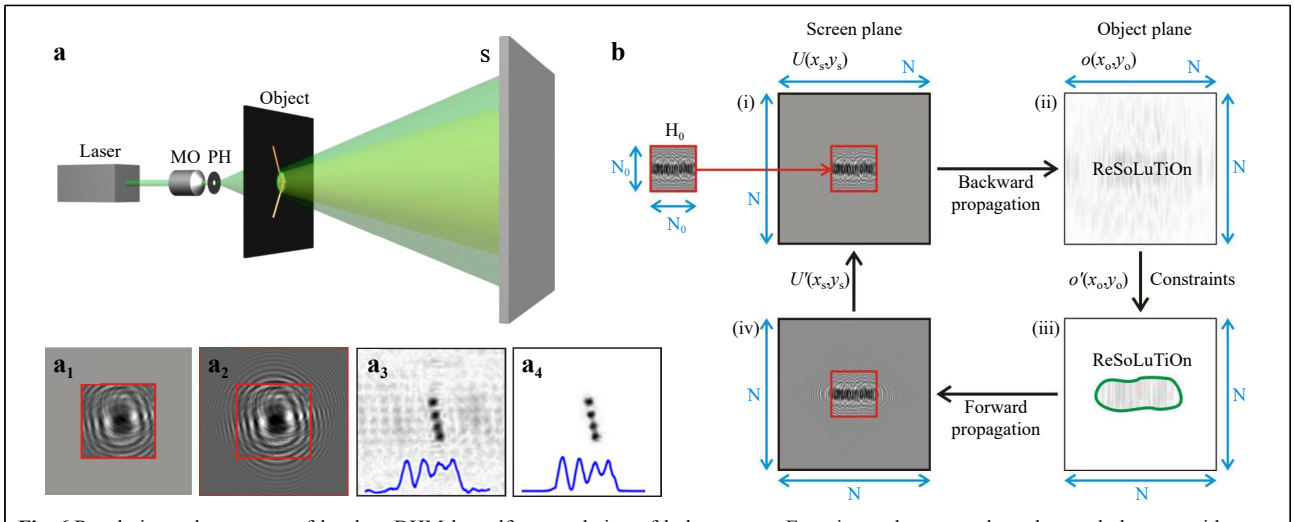

Fig. 6 Resolution enhancement of lensless DHM by self-extrapolation of holograms. **a** Experimental setup and results. a_1, hologram with zero-padding. a_2, hologram after 100 iterations. a_3 and a_4 refer to the reconstructed image without and with self-extrapolation, respectively. **b** Illustration of iterative reconstruction of a hologram by self-extrapolation. The image is adopted from Ref. 104.

retrieved, which has a resolution of $\sigma = \lambda z/(N\Delta_S)$ instead of $\lambda z/(N_0\Delta_S)$. It is clear that the image reconstructed with hologram extrapolation (Fig. $6a_4$) has finer structures than that obtained without using self-extrapolation (Fig. $6a_3$). Quantitatively, the resolution was enhanced from 5.9 μm to 1.8 μm by padding a hologram with 300 × 300 to 1000 × 1000 pixels[108]. The reason for the resolution enhancement by hologram extrapolation is that the hologram itself contains a series of wavelets constituting the wavefront, which can be fitted better through extrapolation and yield a larger effective hologram[104]. This hypothesis is confirmed by a closer look at the intensity distributions ((iv) in Fig. $6a_2$) in the hologram plane.

Hologram synthesis

In addition to inline lensless DHM, DHM, which records the interference between an object wave and an independent reference wave can reconstruct the phase of a sample free of twin-image disturbances. Fig. 7a shows a standard lens-free DHM configuration using an independent reference wave[109,110]. Fig. 7b shows a modified lensless DHM configuration by the insertion of an SLM into the classical Gabor architecture[102]. The SLM is used to perform phase shifting of the *DC* term of the object wave. The complex amplitude distribution of the object wave passing through a sample can be recovered using a standard phase-shifting reconstruction algorithm. For the two types of lens-free DHM configurations (with and without an independent reference wave), the spatial resolution is limited by the size of the hologram, as shown in Eq. 4. In 2002, resolution enhancement of lens-free DHM was first demonstrated[111] by generating an expanded hologram with multiple sub-holograms. Each sub-hologram covers a different frequency spectrum of the input object. When the reconstructed image of each hologram is synthesized, an image with an enlarged FOV and an enhanced spatial resolution can be obtained[109,110]. Generally, hologram synthesis of lens-free DHM can be performed shifting the digital camera[109] or sample[110,112], using oblique beam illuminations[113], or inserting a diffraction grating between the object and digital camera[114,115]. The above-mentioned three strategies are equivalent and generate the same output, which is a larger synthetic hologram that contains a larger sample spectrum.

Figs. 7c–e show the experimental results of the lens-free DHM based on hologram synthesis. The synthesized spectrum is shown in Fig. 7c, and the resolution-enhanced image (Fig. 7e) can be obtained from the Fourier transform of the synthesized spectrum. It is clear that the SA image of the blood cells in Fig. 7e has much finer structures than that in the conventional image in Fig. 7d. Furthermore, it was found that the hologram synthesis enhanced the effective NA from 0.13 to 0.75.

Pixel super-resolution for on-chip DHM

The architecture of a standard on-chip DHM[116–119] is shown in Fig. 8a. A partially coherent light source is used for illumination, usually at > 2–3 cm (z_1 distance) above the sample. A semi-transparent sample is placed on top of an image sensor with a typical spacing of < 1 mm (z_2 distance). As a result, the sample casts an inline hologram, which is directly recorded by a CMOS or CCD image

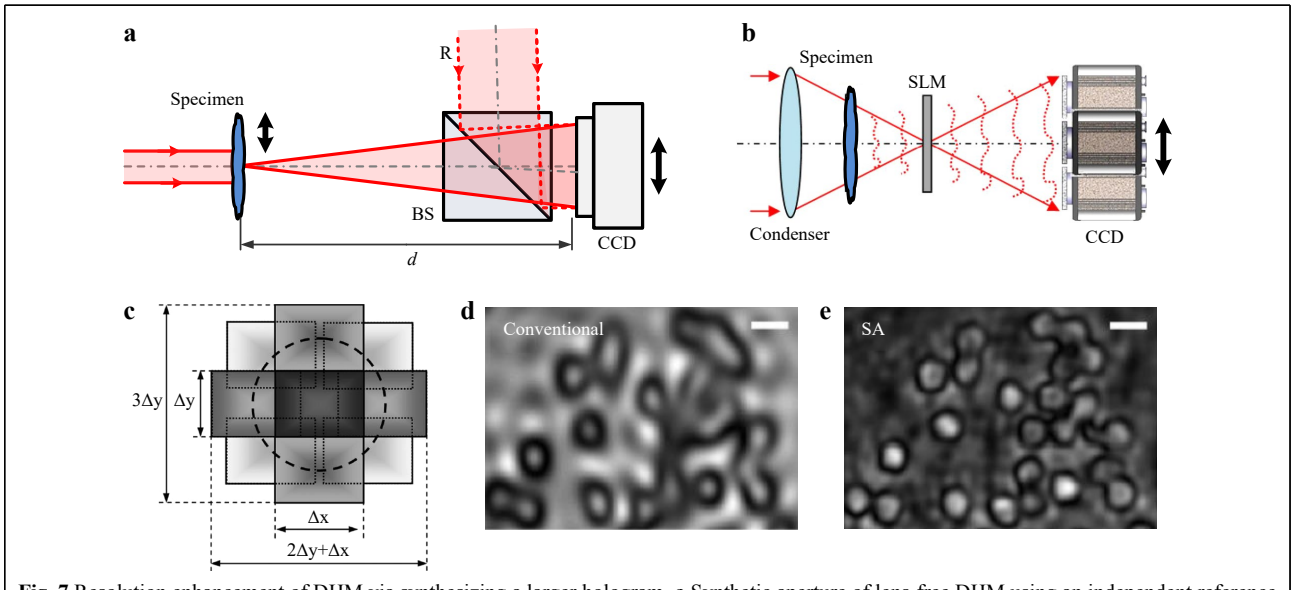

Fig. 7 Resolution enhancement of DHM via synthesizing a larger hologram. **a** Synthetic aperture of lens-free DHM using an independent reference wave. **b** Synthetic aperture of lensless DHM[102], reproduced with permission © IOP Publishing. **c** Synthesized frequency spectrum. **d** and **e**, Images of blood cells without and with applying synthetic aperture, respectively. The images in (**c**–**e**) are adapted from Ref. 113 ©The Optical Society.

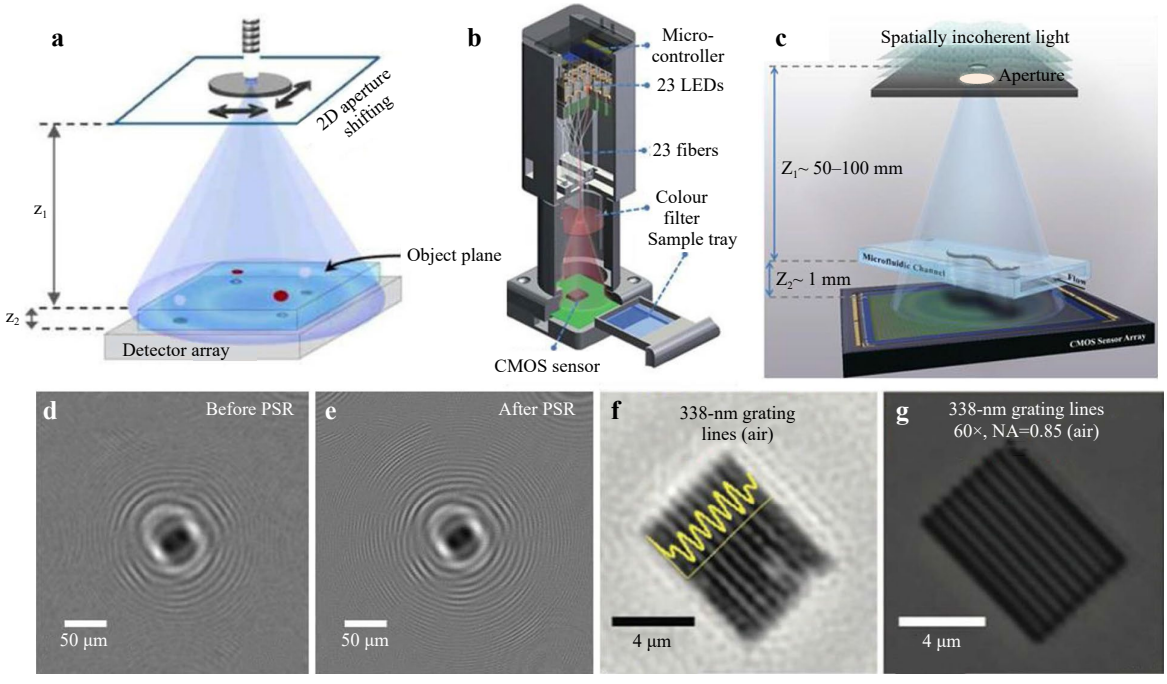

Fig. 8 Pixel super-resolution (PSR) for on-chip lensless DHM. Subpixel shifts in a digital hologram can be achieved through **a** source shifting, **b** an array of static light sources, e.g., fiber-coupled LEDs that are individually controllable, sensor shifting, or **c** sample shifting using e.g., a micro-fluidic flow. **d** An in-line hologram before PSR. **e** Pixel super-resolved hologram of the same object. **f** Reconstructed image of the grating with 338 nm line-width using PSR. **g** Microscope comparison of the same region of interest. The image is adopted from Ref. 118.

sensor, without using any imaging lenses. The magnification time of the on-chip DHM is defined as $M = (z_1 + z_2)/z_1$. For z_1 much larger than z_2, the magnification is approximately 1. The hologram recorded in the on-chip DHM is an in-line hologram (Gabor). The direct reconstruction of object-related holographic information from an inline hologram is often obscured by the twin image and the DC term. Phase retrieval approaches using an iterative approach[7] or additional constraints, such as multiple measurements at different heights[120–123] or illumination angles[124], can be employed to eliminate twin image noise. There are several factors that can limit the resolution of on-chip DHM, including diffraction, pixel size, image chip area, and coherence of the light source. In practice, the primary limitation of lens-free on-chip DHM resolution comes from the pixel size of the sensor (typically 1–2 µm).

To improve the resolution of on-chip DHM, pixel super-resolution (Pixel SR)[125,126] can be adopted by shifting the hologram along the x- and y-directions in subpixel increments. The relative lateral shift of the hologram with respect to the sensor array can also be performed via shifting of the image sensor[127], the illumination source[128] (Fig. 8a, b), or the sample[129] (Fig. 8c), respectively. A low-resolution hologram is captured at each location of the shifted grid. Then, using multiple LR holograms, a higher-resolution hologram can be digitally synthesized by using a "shift-and-add" algorithm, in which the low-resolution (LR) holograms are upsampled, shifted, and digitally added. Alternatively, iterative methods can be used to upsample a high-resolution image from a series of low-resolution images. For this purpose, a cost function can be used for optimization[125]:

$$x^* = \arg\min \sum_i \|W_i \cdot x - y_i\|_p^q + \alpha\gamma(x) \qquad (5)$$

This equation contains two operations, namely, norm and regulation, where i represents the recording times. y_i is a low-resolution hologram, and x is the desired high-resolution image. W_i represents the digital processes of shifting and down-sampling of an image. This synthesis method is equivalent to recording holograms with smaller pixel sizes and higher spatial density detectors. The second part $\gamma(x)$ is a regularization parameter to maintain/regulate the desired quality in the reconstructed image. By solving this optimization function, an image with a pixel size smaller than that of the digital camera can be obtained by synthesizing a series of sub-pixel-shifted LR images. A comparison of Fig. 8d, e shows that PSR can provide a more refined hologram with high-frequency fringes. PSR yields a high-resolution image (Fig. 8f) of a grating (line-

width ~300 nm), whose resolution is equivalent to an effective NA~0.9, as shown in Fig. 8g[116]. Using the PSR techniques, sub-micrometer resolution over a wide FOV of 20–30 mm^2 can be obtained, providing gigapixel throughput with a simple, compact on-chip DHM design[130,131].

Instead of physically moving the image sensor, the light source, or the sample, virtual pinhole scanning completed by deconvolving a hologram with the measured PSF is an alternative way to improve the resolution of an on-chip DHM with an extended light source[132]. PSR can also be performed by varying the propagation distances (i.e., z_2)[133], or by varying the illumination wavelengths in small increments (e.g., 2–3 nm)[134]. To further speed up the sub-hologram recording process by varying the illumination wavelength, color LR holograms can be recorded, where the holograms of the red, reen, and blue illuminations are multiplexed using a sub-pixel shifted Bayer color filter array[119]. Considering that PSR can only enhance the effective NA of the on-chip DHM to 0.9, a synthetic aperture-based on-chip microscope with which the illumination angle is scanned across the surface of a dome (from −50° to 50°) was proposed, which further increased the effective NA to 1.4, achieving a 250-nm resolution at a wavelength of 700-nm across the very large FOV of 20.5 mm^2[124].

Theoretically, an effective NA of 1+n can be achieved in a lensless on-chip DHM using the PSR/SA approach, assuming that the medium between the source and the sample planes is air. Here, n denotes the refractive index of the medium that fills the space between the sample and sensor planes. However, none of these techniques can be considered to exceed the diffraction limit of light, as they are entirely based on propagating waves that result from coherent light-matter interactions.

Deep-learning based methods

Deep-learning[135,136] has been demonstrated as being a powerful tool for solving various inverse problems by training a network with a large quantity of paired images. Deep learning can map the relationship between the input and target output distributions without any prior knowledge of the imaging model. Deep learning has been widely used for holographic image reconstruction[137–139], auto-focusing[140,141], and resolution enhancement[142,143].

The deep-learning configuration for the resolution enhancement of DHM is shown in Fig. 9. By training a set of matched LR and high-resolution images, the relationships between them can be learned. Thus, a high resolution can be retrieved from one or multiple low-resolution images captured by a similar setup. The establishment of the mapping function between the high-resolution output image and the LR input images is called the objective function and is expressed as follows:

$$R_{\text{learn}}=\underset{R_\theta,\theta\in\Theta}{\operatorname{argmin}}\sum_{n=1}^{N}F\left[x_n,R_\theta(y_n)\right]+g(\theta) \tag{6}$$

where R_{learn} is the optimal solution of the weight parameter

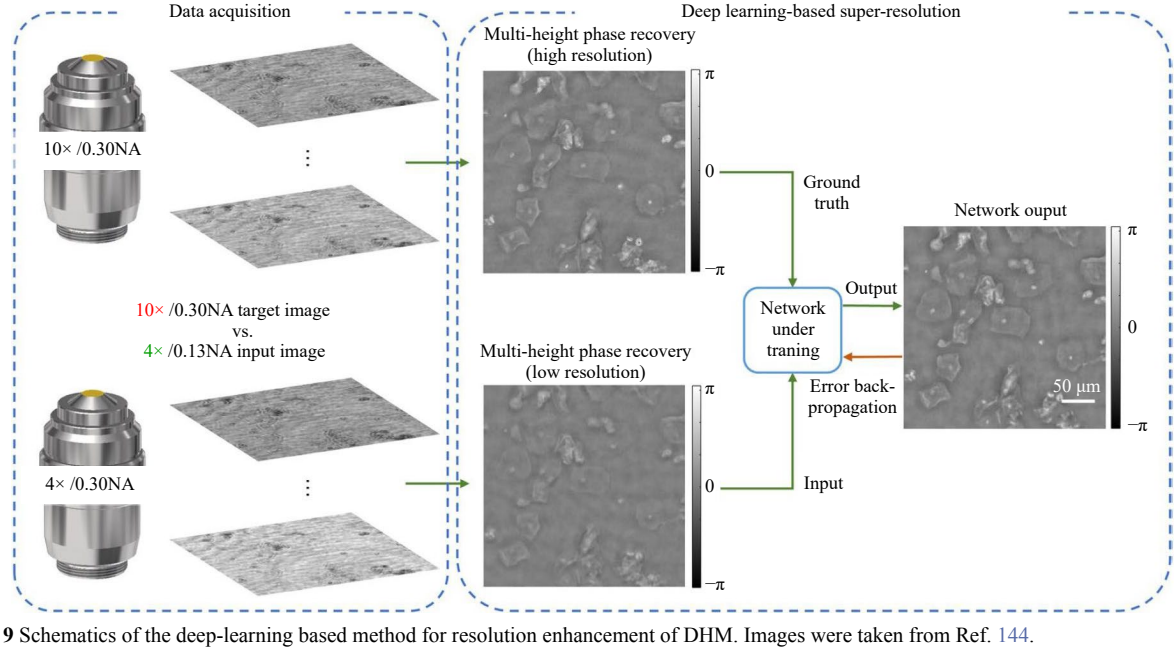

Fig. 9 Schematics of the deep-learning based method for resolution enhancement of DHM. Images were taken from Ref. 144.

of the network, x and y are the training set, F[145] is the loss function for appropriate error metrics, and $g(\theta)$ is a regularization term for the parameter θ to avoid overfitting[146]. By continuously adjusting θ, the error between the output $R_\theta(y_n)$ of the neural network and the target image x_n is minimized. Therefore, as long as the establishment of the model is completed through data statistics, it can be applied to solve inverse problems in imaging. Using the network described in Eq. 6, deep learning has also been used to enhance the resolution of data-driven models for the following two systems: (1) lensless DHM and (2) lens-based DHM systems.

In the first case, a deep learning algorithm based on a generative adversarial network (GAN) must be used in an on-chip lensless DHM to achieve sub-pixel resolution[147]. In this method, the LR reconstructed images are used as inputs and the corresponding high-resolution images of different samples obtained by the "shift-and-add" approach are used as the labels for training the network. A well-trained framework can generate high-resolution images from unseen LR data without an iterative engine and prior knowledge of the system. In 2019, Liu et al. demonstrated that a resolution-improved image could be obtained from much fewer (e.g., 1 or 4 instead of 36 in conventional Pixel SR algorithm) low-resolution sub-pixel-shifted images of the same object by using a neural network, which significantly reduced both the number of hologram measurements and the computation time necessary for reconstruction[144].

The network training process for the lens-based microscopic imaging system is shown in Fig. 8. The reconstructed images of the holograms obtained under the low-magnification objective were used as inputs, and the counterparts obtained under the high-magnification objective were used as labels in the network to generate an image with a resolution of the high-magnification objective, but with the same FOV as of the low-magnification objective [144]. In this way, the diffraction limit defined by the NA of the objective and the SBP of the system can be broken, so that the holographic reconstruction image has a higher resolution and the reconstruction efficiency is improved as compared with the iterative process for each image. A deep-learning-based upscaling method was proposed for overcoming the trade-off between a large FOV and a high resolution, yielding an enlarged hologram with a smaller effective pixel size (enhanced sample details), for which inline holograms are used as training material for the convolutional neural network[148]. In this method, the deep-learning method only uses a single image obtained with a low-NA objective for magnification, allowing detailed analysis of a sample with a high resolution and a large FOV. However, considering that LR-input images do not contain high-resolution components physically, the resolution enhancement capability (or the right guessing of unknown details) of the network is limited by the adequacy of the training data[149]. As a remedy, people tend to integrate deep-learning-based strategies and illumination-modulation techniques to enhance the resolution of DHM. For instance, in 2021, Meng et al. demonstrated that the deep-learning algorithm simplifies[91] not only the resolution-enhanced reconstruction process of SI-DHM but also minimizes the recording requirements[91].

In general, for both lensless DHM and lens-based DHM, a deep-learning-based framework can enlarge the SBP of coherent imaging systems using image data and convolutional neural networks, and provides a rapid, non-iterative method for solving inverse image reconstruction or enhancement problems in optics. Furthermore, it has a faster imaging efficiency, even with little prior knowledge[147], and can reconstruct in real time[150]. This is because deep-learning methods use large-scale datasets to impose potential constraints on the resolution enhancement problem. A neural network has learned millions of weight parameters from a large amount of training data. These parameters can establish a high-dimensional nonlinear relationship between the input and output, which is difficult to express through simple formulas. Although classical principled algorithms are often outperformed by deep learning models, they also retain key advantages. First, classical algorithms inherently produce outputs that are consistent with their inputs because they rely exclusively on the underlying physics and principles formulated. Second, classic algorithms can be generalized for any valid measurement because they are not limited by the adequacy of the training data. Third, classic algorithms, in contrast to deep learning models, do not produce widely erratic outputs after minute tweaks to their inputs.[149]. In light of the above analysis, it is our opinion that deep learning results cannot be blindly trusted, something certainly true of any singular piece of evidence. Incorporating physical models into deep neural networks provides a new idea for expanding the generality and reliability of imaging[151], which should be a new trend in deep learning-based resolution enhancement.

Discussion

In this review, we summarize resolution enhancement approaches for digital holographic microscopy (DHM). Generally, by trading with other degrees of freedom, the spatial resolution is enhanced, and a large field of view (FOV) is preserved (Table 1). Resolution enhancement

Table 1 Overview of Different Resolution enhancement techniques for DHM

Technique/Methods		Features/Capabilities	References
DHM using an imaging lens	Oblique illumination Structured illumination Speckle illumination	• Complex configuration due to the usage of an objective, suffers from objective-related aberration • Achievable resolution: $\sigma = \frac{\kappa_1 \lambda}{NA_{imag}+NA_{illum}}$ • Resolution enhancement factor of 2~5, depending on NA_{illum}/NA_{imag}. • FOV is limited by the objective design: 1x1 mm^2 under a 10× objective, etc.	49, 77, 96
DHM without using an imaging lens	Self-extrapolation of holograms	• No extra measurement is needed • Achievable resolution is $\lambda z/(N\Delta_S)$ instead of $\lambda z/(N_0\Delta_S)$, when the hologram is effectively extrapolated from $N_0\Delta_S$ to $N\Delta_S$.	104, 106-108
	Hologram expansion by shifting the CCD or the sample	• Achievable resolution: $\delta=\lambda z/L_{hologram}$ • Effective NA up to 0.3, and FOV: up to 20×16 mm^2	110, 112, 113
	Pixel super-resolution for on-chip DHM	• Subpixel-shifts (e.g.,6×6) of hologram yields an NA of 0.9 • Oblique illumination further enhances NA to 1.4 and improves the SNR. • FOV up to 20 mm^2	116, 118, 125, 128, 129124
AI algorithm based techniques	Deep-learning	• Relies on large-scale data sets, time-consuming. • Reconstruction can be wrong if the training data is inadequate. • Resolution is diffraction limited.	144,148

approaches can be classified into two categories, namely, lens-based DHM and lens-free DHM, based on whether an objective lens is used. In lens-based DHM, oblique illumination, structured illumination, and speckle illumination were used to enhance the spatial resolution of DHM. In sample-distant lens-free DHM, self-extrapolation of holograms can enhance the physical-aperture-limited spatial resolution. Furthermore, the resolution can be further enhanced by synthesizing a larger hologram by scanning the sample, camera, illumination, or inserting a diffraction grating between the sample and the camera. With a lens-free on-chip DHM, resolution enhancement can be obtained by pixel super-resolution and a synthetic aperture by shifting the illumination beam. Recently, deep learning has also been used to enhance the resolution in DHM. Being trained with plenty experimental datasets obtained under well-controlled imaging conditions, deep neural networks enable the enhancement of the spatial resolution or the SBP of DHM in a rapid, non-iterative manner. It is worth pointing out that the resolution enhancement approaches in DHM can surpass the resolution limited by the geometry (NA) of the imaging system in terms of 0.82λ/NA. However, they cannot surpass the physical diffraction limit λ(2NA)[152] in far-field imaging.

In the past decade, intensive efforts have been made to achieve coherent imaging resolution beyond the diffraction limit. There are two coherent imaging approaches that can achieve super-resolution capability. The first is synthetic-aperture DHM using evanescent waves, which can exceed the diffraction limit in the near-field region. The second is super-oscillation illumination or super-oscillatory lens-based optical microscopy[153]. We envisage that there will be an increasing number of investigations concerning the physics of DHM resolution enhancement, and these investigations will widen the applications of DHM in different fields.

Acknowledgements
The authors acknowledge the support from the National Key Research and Development Program of China (2021YFF0700300), the National Natural Science Foundation of China (NSFC 62075177, 62175112), the Natural Science Foundation of Shaanxi Province (2020JM-193 and 2020JQ-324), and the Fundamental Research Funds for the Central Universities (XJS210503, XJS210504, JC2112, and JB210513).

Author details
[1]School of Physics and Optoelectronic Engineering, Xidian University, Xi'an 710071, China. [2]Academy of Advanced Interdisciplinary research, Xidian University, Xi 'an 710071, China. [3]Key Laboratory for Opto-Electronic Technology of Jiangsu Province, Nanjing Normal University, Nanjing 210023, China

Conflict of interest
The authors declare that they have no conflict of interest.

Received: 03 September 2021 Revised: 18 January 2022 Accepted: 19 January 2022
Accepted article preview online: 21 January 2022
Published online: 27 January 2022

References

1. Schnars, U. & Jüptner, W. Direct recording of holograms by a CCD target and numerical reconstruction. *Applied Optics* **33**, 179-181 (1994).
2. Yu, X. et al. Review of digital holographic microscopy for three-dimensional profiling and tracking. *Optical Engineering* **53**, 112306 (2014).
3. Osten, W. et al. Recent advances in digital holography [Invited]. *Applied Optics* **53**, G44-G63 (2014).
4. Micó, V. et al. Resolution enhancement in quantitative phase microscopy. *Advances in Optics and Photonics* **11**, 135-214 (2019).
5. Goodman, J. W. & Lawrence, R. W. Digital image formation from electronically detected holograms. *Applied Physics Letters* **11**, 77-79 (1967).
6. Kim, M. K. Principles and techniques of digital holographic microscopy. *SPIE Reviews* **1**, 018005 (2010).
7. Latychevskaia, T. & Fink, H. W. Solution to the twin image problem in holography. *Physical Review Letters* **98**, 233901 (2007).
8. Gabor, D. A new microscopic principle. *Nature* **161**, 777-778 (1948).
9. Langehanenberg, P., von Bally, G. & Kemper, B. Autofocusing in digital holographic microscopy. *3D Research* **2**, 4 (2011).
10. Gao, P. et al. Autofocusing of digital holographic microscopy based on off-axis illuminations. *Optics Letters* **37**, 3630-3632 (2012).
11. Charrière, F. et al. Characterization of microlenses by digital holographic microscopy. *Applied Optics* **45**, 829-835 (2006).
12. Markus, F. et al. Digital holography in production: an overview. *Light:Advanced Manufacturing* **2**, 15 (2021).
13. Cubreli, G. et al. Digital holographic interferometry for the measurement of symmetrical temperature fields in liquids. *Photonics* **8**, 200 (2021).
14. Kemper, B. & von Bally, G. Digital holographic microscopy for live cell applications and technical inspection. *Applied Optics* **47**, A52-A61 (2008).
15. Born, M. & Wolf, E. Principles of Optics. 7th edn. (Cambridge: Cambridge University, 1999).
16. Cotte, Y. et al. Marker-free phase nanoscopy. *Nature Photonics* **7**, 113-117 (2013).
17. den Dekker, A. J. & van den Bos. A. Resolution: a survey. *Journal of the Optical Society of America A* **14**, 547-557 (1997).
18. Faridian, A. et al. Nanoscale imaging using deep ultraviolet digital holographic microscopy. *Optics Express* **18**, 14159-14164 (2010).
19. Lohmann, A. W. et al. Space-bandwidth product of optical signals and systems. *Journal of the Optical Society of America A* **13**, 470-473 (1996).
20. Cox, I. J. & Sheppard, C. J. R. Information capacity and resolution in an optical system. *Journal of the Optical Society of America A* **3**, 1152-1158 (1986).
21. Zheng, G. A., Horstmeyer, R. & Yang, C. H. Wide-field, high-resolution Fourier ptychographic microscopy. *Nature Photonics* **7**, 739-745 (2013).
22. Micó, V., Zalevsky, Z. & García, J. Optical superresolution: imaging beyond abbe's diffraction limit. *Journal of Holography and Speckle* **5**, 110-123 (2009).
23. Zalevsky, Z., Micó, V. & Garcia, J. Nanophotonics for optical super resolution from an information theoretical perspective: a review. *Journal of Nanophotonics* **3**, 032502 (2009).
24. Ueda, M. & Sato, T. Superresolution by holography. *Journal of the Optical Society of America* **61**, 418-419 (1971).
25. Ueda, M., Sato, T. & Kondo, M. Superresolution by multiple superposition of image holograms having different carrier frequencies. *Optica Acta:International Journal of Optics* **20**, 403-410 (1973).
26. Sato, T., Ueda, M. & Yamagish, G. Superresolution microscope using electrical superposition of holograms. *Applied Optics* **13**, 406-408 (1974).
27. Sato, T., Ueda, M. & Ikeda, T. Real time superresolution by means of an ultrasonic light diffractor and TV system. *Applied Optics* **13**, 1318-1321 (1974).
28. Kuznetsova, Y., Neumann, A. & Brueck, S. R. J. Imaging interferometric microscopy. *Journal of the Optical Society of America A* **25**, 811-822 (2008).
29. Neumann, A., Kuznetsova, Y. & Brueck, S. R. J. Optical resolution below λ/4 using synthetic aperture microscopy and evanescent-wave illumination. *Optics Express* **16**, 20477-20483 (2008).
30. Micó, V. et al. Superresolution digital holographic microscopy for three-dimensional samples. *Optics Express* **16**, 19260-19270 (2008).
31. Hillman, T. R. et al. High-resolution, wide-field object reconstruction with synthetic aperture Fourier holographic optical microscopy. *Optics Express* **17**, 7873-7892 (2009).
32. Bühl, J. et al. Digital synthesis of multiple off-axis holograms with overlapping Fourier spectra. *Optics Communications* **283**, 3631-3638 (2010).
33. Gutzler, T. et al. Coherent aperture-synthesis, wide-field, high-resolution holographic microscopy of biological tissue. *Optics Letters* **35**, 1136-1138 (2010).
34. Granero, L. et al. Single-exposure super-resolved interferometric microscopy by RGB multiplexing in lensless configuration. *Optics and Lasers in Engineering* **82**, 104-112 (2016).
35. Calabuig, A. et al. Single-exposure super-resolved interferometric microscopy by red-green-blue multiplexing. *Optics Letters* **36**, 885-887 (2011).
36. Calabuig, A. et al. Resolution improvement by single-exposure superresolved interferometric microscopy with a monochrome sensor. *Journal of the Optical Society of America A* **28**, 2346-2358 (2011).
37. Choi, Y. et al. Synthetic aperture microscopy for high resolution imaging through a turbid medium. *Optics Letters* **36**, 4263-4265 (2011).
38. Yuan, C. J. et al. Resolution improvement in digital holography by angular and polarization multiplexing. *Applied Optics* **50**, B6-B11 (2011).
39. Picazo-Bueno, J. Á. et al. Superresolved spatially multiplexed interferometric microscopy. *Optics Letters* **42**, 927-930 (2017).
40. Mico, V. et al. Synthetic aperture superresolution with multiple off-axis holograms. *Journal of the Optical Society of America A* **23**, 3162-3170 (2006).
41. Kim, M. et al. High-speed synthetic aperture microscopy for live cell imaging. *Optics Letters* **36**, 148-150 (2011).
42. Micó, V., Zalevsky, Z. & Garcia, J. Superresolved common-path phase-shifting digital inline holographic microscopy using a spatial light modulator. *Optics Letters* **37**, 4988-4990 (2012).
43. Kuznetsova, Y., Neumann, A. & Brueck, S. R. J. Imaging interferometric microscopy - approaching the linear systems limits of optical resolution. *Optics Express* **15**, 6651-6663 (2007).
44. Mico, V., Zalevsky, Z. & García, J. Synthetic aperture microscopy using off-axis illumination and polarization coding. *Optics Communications* **276**, 209-217 (2007).
45. Indebetouw, G. et al. Scanning holographic microscopy with resolution exceeding the Rayleigh limit of the objective by superposition of off-axis holograms. *Applied Optics* **46**, 993-1000 (2007).
46. Mico, V. et al. Superresolved imaging in digital holography by superposition of tilted wavefronts. *Applied Optics* **45**, 822-828 (2006).
47. Mico, V. et al. Single-step superresolution by interferometric imaging.

Optics Express **12**, 2589-2596 (2004).
48. Indebetouw, G., El Maghnouji, A. & Foster, R. Scanning holographic microscopy with transverse resolution exceeding the Rayleigh limit and extended depth of focus. *Journal of the Optical Society of America A* **22**, 892-898 (2005).
49. Cheng, C. J. et al. Superresolution imaging in synthetic aperture digital holographic microscopy. Proceedings of the IEEE 4th International Conference on Photonics. Melaka: IEEE, 2013.
50. Schwarz, C. J., Kuznetsova, Y. & Brueck, S. R. J. Imaging interferometric microscopy. *Optics Letters* **28**, 1424-1426 (2003).
51. Lee, D. J. & Weiner, A. M. Optical phase imaging using a synthetic aperture phase retrieval technique. *Optics Express* **22**, 9380-9394 (2014).
52. Mico, V. et al. Transverse resolution improvement using rotating-grating time-multiplexing approach. *Journal of the Optical Society of America A* **25**, 1115-1129 (2008).
53. Lin, Y. C. et al. One-shot synthetic aperture digital holographic microscopy with non-coplanar angular-multiplexing and coherence gating. *Optics Express* **26**, 12620-12631 (2018).
54. Hussain, A. et al. Simple fringe illumination technique for optical superresolution. *Journal of the Optical Society of America B* **34**, B78-B84 (2017).
55. Hussain, A. et al. Super resolution imaging achieved by using on-axis interferometry based on a Spatial Light Modulator. *Optics Express* **21**, 9615-9623 (2013).
56. Mudassar, A. A. A simplified holography based superresolution system. *Optics and Lasers in Engineering* **75**, 27-38 (2015).
57. Hussain, A. & Mudassar, A. A. Optical super resolution using tilted illumination coupled with object rotation. *Optics Communications* **339**, 34-40 (2015).
58. Hussain, A. & Mudassar, A. A. Holography based super resolution. *Optics Communications* **285**, 2303-2310 (2012).
59. Phan, A. H., Park, J. H. & Kim, N. Super-resolution digital holographic microscopy for three dimensional sample using multipoint light source illumination. *Japanese Journal of Applied Physics* **50**, 092503 (2011).
60. Mudassar, A. A. & Hussain, A. Super-resolution of active spatial frequency heterodyning using holographic approach. *Applied Optics* **49**, 3434-3441 (2010).
61. Micó, V., García, J. & Zalevsky, Z. Axial superresolution by synthetic aperture generation. *Journal of Optics A:Pure and Applied Optics* **10**, 125001 (2008).
62. Micó, V., Zalevsky, Z. & García, J. Edge processing by synthetic aperture superresolution in digital holographic microscopy. *3D Research* **2**, 1 (2011).
63. Kim, M. et al. Three-dimensional differential interference contrast microscopy using synthetic aperture imaging. *Journal of Biomedical Optics* **17**, 026003 (2012).
64. Gao, P. et al. Phase-shifting Zernike phase contrast microscopy for quantitative phase measurement. *Optics Letters* **36**, 4305-4307 (2011).
65. Wolf, E. Three-dimensional structure determination of semi-transparent objects from holographic data. *Optics Communications* **1**, 153-156 (1969).
66. Kim, K., Yoon, J. & Park, Y. Large-scale optical diffraction tomography for inspection of optical plastic lenses. *Optics Letters* **41**, 934-937 (2016).
67. Charrière, F. et al. Living specimen tomography by digital holographic microscopy: morphometry of testate amoeba. *Optics Express* **14**, 7005-7013 (2006).
68. Kim, K., Yoon, J. & Park, Y. Simultaneous 3D visualization and position tracking of optically trapped particles using optical diffraction tomography. *Optica* **2**, 343-346 (2015).
69. Chen, M. et al. Multi-layer Born multiple-scattering model for 3D phase microscopy. *Optica* **7**, 394-403 (2020).
70. Isikman, S. O. et al. Lens-free optical tomographic microscope with a large imaging volume on a chip. *Proceedings of the National Academy of Sciences of the United States of America* **108**, 7296-7301 (2011).
71. Wang, J. et al. Airy-beam tomographic microscopy. *Optica* **7**, 790-793 (2020).
72. Kuś, A. Real-time, multiplexed holographic tomography. *Optics and Lasers in Engineering* **149**, 106783 (2022).
73. Kamilov, U. S. et al. Learning approach to optical tomography. *Optica* **2**, 517-522 (2015).
74. Gustafsson, M. G. L. Surpassing the lateral resolution limit by a factor of two using structured illumination microscopy. *Journal of Microscopy* **198**, 82-87 (2000).
75. Gustafsson, M. G. L. Nonlinear structured-illumination microscopy: wide-field fluorescence imaging with theoretically unlimited resolution. *Proceedings of the National Academy of Sciences of the United States of America* **102**, 13081-13086 (2005).
76. Gao, P., Pedrini, G. & Osten, W. Structured illumination for resolution enhancement and autofocusing in digital holographic microscopy. *Optics Letters* **38**, 1328-1330 (2013).
77. Chowdhury, S. et al. Refractive index tomography with structured illumination. *Optica* **4**, 537-545 (2017).
78. Sánchez-Ortiga, E. et al. Enhancing spatial resolution in digital holographic microscopy by biprism structured illumination. *Optics Letters* **39**, 2086-2089 (2014).
79. Lee, K. et al. Time-multiplexed structured illumination using a DMD for optical diffraction tomography. *Optics Letters* **42**, 999-1002 (2017).
80. Hussain, A. & Fuentes, J. L. M. Resolution enhancement using simultaneous couple illumination. *Journal of Optics* **18**, 105702 (2016).
81. Ganjkhani, Y. et al. Super-resolved Mirau digital holography by structured illumination. *Optics Communications* **404**, 110-117 (2017).
82. Yuan, C. J. et al. Resolution enhancement of the microscopic imaging by unknown sinusoidal structured illumination with iterative algorithm. *Applied Optics* **56**, F78-F83 (2017).
83. Yeh, L. H., Tian, L. & Waller, L. Structured illumination microscopy with unknown patterns and a statistical prior. *Biomedical Optics Express* **8**, 695-711 (2017).
84. Zheng, J. J. et al. Digital holographic microscopy with phase-shift-free structured illumination. *Photonics Research* **2**, 87-91 (2014).
85. Chowdhury, S. & Izatt, J. Structured illumination diffraction phase microscopy for broadband, subdiffraction resolution, quantitative phase imaging. *Optics Letters* **39**, 1015-1018 (2014).
86. Lai, X. J. et al. Coded aperture structured illumination digital holographic microscopy for superresolution imaging. *Optics Letters* **43**, 1143-1146 (2018).
87. Chowdhury, S. & Izatt, J. Structured illumination quantitative phase microscopy for enhanced resolution amplitude and phase imaging. *Biomedical Optics Express* **4**, 1795-1805 (2013).
88. Yuan, C. J., Feng, S. T. & Nie, S. P. Digital holographic microscopy by using structured illumination. *Chinese Journal of Lasers* **43**, 0609003 (2016).
89. Li, S. H. et al. Phase-shifting-free resolution enhancement in digital holographic microscopy under structured illumination. *Opt Express* **26**, 23572-23584 (2018).
90. Chowdhury, S. et al. Structured illumination multimodal 3D-resolved quantitative phase and fluorescence sub-diffraction microscopy. *Biomedical Optics Express* **8**, 2496-2518 (2017).

91. Meng, Z. et al. DL-SI-DHM: a deep network generating the high-resolution phase and amplitude images from wide-field images. *Optics Express* **29**, 19247-19261 (2021).
92. Shin, S. et al. Active illumination using a digital micromirror device for quantitative phase imaging. *Optics Letters* **40**, 5407-5410 (2015).
93. Goodman, J. W. Speckle Phenomena in Optics: Theory and Applications. (Englewood: Roberts & Co, 2006).
94. García, J., Zalevsky, Z. & Fixler, D. Synthetic aperture superresolution by speckle pattern projection. *Optics Express* **13**, 6073-6078 (2005).
95. Zheng, J. J. et al. Autofocusing and resolution enhancement in digital holographic microscopy by using speckle-illumination. *Journal of Optics* **17**, 085301 (2015).
96. Park, Y. et al. Speckle-field digital holographic microscopy. *Optics Express* **17**, 12285-12292 (2009).
97. Liu, Y. et al. Dynamic speckle illumination digital holographic microscopy by doubly scattered system. *Photonics* **8**, 276 (2021).
98. Yilmaz, H. et al. Speckle correlation resolution enhancement of wide-field fluorescence imaging. *Optica* **2**, 424-429 (2015).
99. Choi, Y. et al. Overcoming the diffraction limit using multiple light scattering in a highly disordered medium. *Physical Review Letters* **107**, 023902 (2011).
100. Baek, Y., Lee, K. & Park, Y. High-resolution holographic microscopy exploiting speckle-correlation scattering matrix. *Physical Review Applied* **10**, 024053 (2018).
101. Repetto, L., Piano, E. & Pontiggia, C. Lensless digital holographic microscope with light-emitting diode illumination. *Optics Letters* **29**, 1132-1134 (2004).
102. Micó, V. et al. Superresolved phase-shifting Gabor holography by CCD shift. *Journal of Optics A:Pure and Applied Optics* **11**, 125408 (2009).
103. Miao, J., Sayre, D. & Chapman, H. N. Phase retrieval from the magnitude of the Fourier transforms of nonperiodic objects. *Journal of the Optical Society of America A* **15**, 1662-1669 (1998).
104. Latychevskaia, T. & Fink, H. W. Resolution enhancement in digital holography by self-extrapolation of holograms. *Optics Express* **21**, 7726-7733 (2013).
105. Zhang, W. H. et al. Twin-image-free holography: a compressive sensing approach. *Physical Review Letters* **121**, 093902 (2018).
106. Rong, L. et al. Terahertz in-line digital holography of dragonfly hindwing: amplitude and phase reconstruction at enhanced resolution by extrapolation. *Optics Express* **22**, 17236-17245 (2014).
107. Rong, L. et al. Terahertz in-line digital holography of human hepatocellular carcinoma tissue. *Scientific Reports* **5**, 8445 (2015).
108. Latychevskaia, T. & Fink, H. W. Coherent microscopy at resolution beyond diffraction limit using post-experimental data extrapolation. *Applied Physics Letters* **103**, 204105 (2013).
109. Di, J. L. et al. High resolution digital holographic microscopy with a wide field of view based on a synthetic aperture technique and use of linear CCD scanning. *Applied Optics* **47**, 5654-5659 (2008).
110. Micó, V., Ferreira, C. & García, J. Surpassing digital holography limits by lensless object scanning holography. *Optics Express* **20**, 9382-9395 (2012).
111. Massig, J. H. Digital off-axis holography with a synthetic aperture. *Optics Letters* **27**, 2179-2181 (2002).
112. Bianco, V., Paturzo, M. & Ferraro, P. Spatio-temporal scanning modality for synthesizing interferograms and digital holograms. *Optics Express* **22**, 22328-22339 (2014).
113. Granero, L. et al. Synthetic aperture superresolved microscopy in digital lensless Fourier holography by time and angular multiplexing of the object information. *Applied Optics* **49**, 845-857 (2010).
114. Paturzo, M. et al. Super-resolution in digital holography by a two-dimensional dynamic phase grating. *Optics Express* **16**, 17107-17118 (2008).
115. Liu, C. Super-resolution digital holographic imaging method. *Applied Physics Letters* **81**, 3143-3145 (2002).
116. Greenbaum, A. et al. Imaging without lenses: achievements and remaining challenges of wide-field on-chip microscopy. *Nature Methods* **9**, 889-895 (2012).
117. Mudanyali, O. et al. Compact, light-weight and cost-effective microscope based on lensless incoherent holography for telemedicine applications. *Lab on A Chip* **10**, 1417-1428 (2010).
118. Wu, Y. C. & Ozcan, A. Lensless digital holographic microscopy and its applications in biomedicine and environmental monitoring. *Methods* **136**, 4-16 (2018).
119. Wu, Y. C. et al. Demosaiced pixel super-resolution for multiplexed holographic color imaging. *Scientific Reports* **6**, 28601 (2016).
120. Mitome, M. Transport of intensity equation method and its applications, Microscopy, 70, 69–74 (2021).
121. Pedrini, G., Osten, W. & Zhang, Y. Wave-front reconstruction from a sequence of interferograms recorded at different planes. *Optics Letters* **30**, 833-835 (2005).
122. Allen, L. J. & Oxley, M. P. Phase retrieval from series of images obtained by defocus variation. *Optics Communications* **199**, 65-75 (2001).
123. Fienup, J. R. Reconstruction of an object from the modulus of its Fourier transform. *Optics Letters* **3**, 27-29 (1978).
124. Luo, W. et al. Synthetic aperture-based on-chip microscopy. *Light:Science & Applications* **4**, e261 (2015).
125. Bishara, W. et al. Lensfree on-chip microscopy over a wide field-of-view using pixel super-resolution. *Optics Express* **18**, 11181-11191 (2010).
126. Farsiu, S. et al. Fast and robust multiframe super resolution. *IEEE Transactions on Image Processing* **13**, 1327-1344 (2004).
127. Greenbaum, A. et al. Wide-field computational imaging of pathology slides using lens-free on-chip microscopy. *Science Translational Medicine* **6**, 267ra175 (2014).
128. Bishara, W. et al. Holographic pixel super-resolution in portable lensless on-chip microscopy using a fiber-optic array. *Lab on A Chip* **11**, 1276-1279 (2011).
129. Bishara, W., Zhu, H. Y. & Ozcan, A. Holographic opto-fluidic microscopy. *Optics Express* **18**, 27499-27510 (2010).
130. McLeod, E. et al. *Toward giga-pixel nanoscopy on a chip*: a computational wide-field look at the nano-scale without the use of lenses. *Lab on A Chip* **13**, 2028-2035 (2013).
131. Greenbaum, A. et al. Increased space-bandwidth product in pixel super-resolved lensfree on-chip microscopy. *Scientific Reports* **3**, 1717 (2013).
132. Feng, S. D. & Wu, J. G. Resolution enhancement method for lensless in-line holographic microscope with spatially-extended light source. *Optics Express* **25**, 24735-24744 (2017).
133. Wang, H. D. et al. Computational out-of-focus imaging increases the space–bandwidth product in lens-based coherent microscopy. *Optica* **3**, 1422-1429 (2016).
134. Luo, W. et al. Pixel super-resolution using wavelength scanning. *Light:Science & Applications* **5**, e16060 (2016).
135. LeCun, Y., Bengio, Y. & Hinton, G. Deep learning. *Nature* **521**, 436-444 (2015).
136. Ongie, G. et al. Deep learning techniques for inverse problems in imaging. *IEEE Journal on Selected Areas in Information Theory* **1**, 39-56 (2020).
137. Rivenson, Y., Wu, Y. C. & Ozcan, A. Deep learning in holography and coherent imaging. *Light:Science & Applications* **8**, 85 (2019).
138. Zhang, G. et al. Fast phase retrieval in off-axis digital holographic microscopy through deep learning. *Optics Express* **26**, 19388-19405

(2018).
139. Xiao, W. et al. Adaptive frequency filtering based on convolutional neural networks in off-axis digital holographic microscopy. *Biomedical Optics Express* **10**, 1613-1626 (2019).
140. Rivenson, Y. et al. Phase recovery and holographic image reconstruction using deep learning in neural networks. *Light:Science & Applications* **7**, 17141 (2018).
141. Ding, H. et al. Auto-focusing and quantitative phase imaging using deep learning for the incoherent illumination microscopy system. *Optics Express* **29**, 26385-26403 (2021).
142. Rivenson, Y. et al. Deep learning microscopy. *Optica* **4**, 1437-1443 (2017).
143. Nehme, E. et al. Deep-STORM: super-resolution single-molecule microscopy by deep learning. *Optica* **5**, 458-464 (2018).
144. Liu, T. R. et al. Deep learning-based super-resolution in coherent imaging systems. *Scientific Reports* **9**, 3926 (2019).
145. Ghosh, N. & Bhattacharya, K. Cube beam-splitter interferometer for phase shifting interferometry. *Journal of Optics* **38**, 191-198 (2009).
146. McCann, M. T., Jin, K. H. & Unser, M. Convolutional neural networks for inverse problems in imaging: a review. *IEEE Signal Processing Magazine* **34**, 85-95 (2017).
147. Barbastathis, G., Ozcan, A. & Situ, G. On the use of deep learning for computational imaging. *Optica* **6**, 921-943 (2019).
148. Byeon, H., Go, T. & Lee, S. J. Deep learning-based digital in-line holographic microscopy for high resolution with extended field of view. *Optics & Laser Technology* **113**, 77-86 (2019).
149. Belthangady, C. & Royer, L. A. Applications, promises, and pitfalls of deep learning for fluorescence image reconstruction. *Nature Methods* **16**, 1215-1225 (2019).
150. de Haan, K. et al. Deep-learning-based image reconstruction and enhancement in optical microscopy. *Proceedings of the IEEE* **108**, 30-50 (2020).
151. Wang, F. et al. Phase imaging with an untrained neural network. *Light:Science & Applications* **9**, 77 (2020).
152. Goodman, J. W. Introduction to Fourier Optics. 3rd edn. (Greenwoood Village: Roberts & Company Publishers, 2005).
153. Rogers, E. T. F. et al. A super-oscillatory lens optical microscope for subwavelength imaging. *Nature Materials* **11**, 432-435 (2012).